

Contribution to the Application of the Robust Control Multivariable Systems to an Aerogenerator Dfim Type

Randrianambinintsoa Manitra Léon¹, Randriamitantsoa Paul Auguste²

¹ PhDStudent, GE, ED-STII, Université d'Antananarivo Madagascar,
² ThesisDirector, TASI, ED-STII, Université d'Antananarivo Madagascar,

Submitted: 10-10-2021

Revised: 19-10-2021

Accepted: 22-10-2021

ABSTRACT: This article presents the research results of a DFIM behavior (Double Fed Induction Machine), for the electrical energy production by a wind generator system, by the directly integrating its model, its direct simulation in order to present its behavior, in order to make tuning and present the desired behavior. The objectives being to contribute to its modeling, then to adjust and analyze a DFIM type wind turbine generator for applying the robust control of the multivariable system. In a brief way, the essential aim is to control the machine for generate electrical energy by controlling the powers by the currents and voltages rotor, while regulating its speed rotation.

KEY WORDS: DFIM, electric control systems, electric machines, robust control system, wind turbines,

I. INTRODUCTION

In the current era, the performance and reliability of wind energy, as well as the continuity of its service, should replace the production of old-fashioned electrical energy which is increasingly creating climatic destabilization phenomena due to the polluting gases emission. One of the more specific configurations of variable speed wind turbines, uses

the asynchronous double fed machine, referred to by the abbreviation DFIM or MADA (Machine Asynchrone à Double Alimentation) in French. Many of the DFIM control strategies have been proposed in literature. The problem of the DFIM control strategy has been dealt with using different approaches. The DFIM oriented field control, with and without speed sensor, has been presented (Metwally et al. (2002) and EL Khil de Khojet et al. 2004). The lack tolerance of the DFIM command has been studied under time-varying conditions (Gritli et al. 2011). Other control strategies including direct torque control (Bonnet et al. 2007), sliding-mode control (Vidal et al. 2008), output-feedback control (Peresadaa et al. 2004), and closed loop control (Salloum et al. 2007) [1].

II. PRESENTATION OF THE PROBLEM

A. System model to order

The machine is controlled to generate electrical energy by controlling the powers by the rotor currents and voltages, while regulating its rotation speed. The call of tools for solving mathematical differential equations allows modeling of machine dynamics under differential equations systems. We have the following parameters, [2] [3]:

$$\gamma_1 = \frac{R_r L_s^2 + R_s M_{sr}^2}{\sigma L_r L_s^2}, \quad \gamma_2 = \frac{M_{sr}}{\sigma L_s L_r}, \quad \gamma_3 = \frac{1}{\sigma L_r}, \quad \sigma = 1 - \frac{M_{sr}^2}{L_s L_r}, \quad \tau_s = \frac{L_s}{R_s}$$

$$v_{rd} = u_1 v_{dc}, \quad v_{rq} = u_2 v_{dc} \quad i_e = u_1 i_{rd} + u_1 i_{rq} \quad i_{ot} = u_3 i_{red} + u_4 i_{req}$$

$$\left\{ \begin{aligned}
 \frac{d\omega_m}{dt} &= -\frac{F}{J}\omega_m - p\frac{M_{sr}}{JL_s}(\phi_{sd}i_{rd} - \phi_{sd}i_{rq}) - \frac{T_L}{J} \\
 \frac{di_{sd}}{dt} &= -\gamma_{sd}i_{sd} + \omega_s i_{sq} + p\omega_m \frac{M_{sr}}{\sigma L_s L_r} \phi_r + \frac{1}{\sigma L_s} v_{sd} \\
 \frac{di_{sq}}{dt} &= -\gamma_{sq}i_{sq} + \omega_s i_{sd} + p\omega_m \frac{M_{sr}}{\sigma L_s L_r} \phi_r + \frac{1}{\sigma L_s} v_{sq} \\
 \frac{di_{rd}}{dt} &= -\gamma_1 i_{rd} + (\omega_s - p\omega_m)i_{rq} + \frac{\gamma_2}{\tau_s} \phi_{sq} - p\gamma_2 \omega_m \phi_{sq} - \gamma_2 V_s \\
 &+ \gamma_3 v_{dc} u_1 \\
 \frac{di_{rq}}{dt} &= -\gamma_1 i_{rq} - (\omega_s - p\omega_m)i_{rd} + \frac{\gamma_2}{\tau_s} \phi_{sq} + p\gamma_2 \omega_m \phi_{sd} \\
 &+ \gamma_3 v_{dc} u_2 \\
 \frac{dv_{dc}}{dt} &= \frac{1}{C}(u_3 i_{red} + u_4 i_{req} - i_e) \\
 \frac{di_{red}}{dt} &= \omega_s i_{req} + \frac{V_s}{L_0} - \frac{v_{dc} u_3}{L_0} \\
 \frac{di_{req}}{dt} &= -\omega_s i_{red} - \frac{v_{dc} u_4}{L_0}
 \end{aligned} \right. \quad (1)$$

Possibilities control of the machine are presented in figure 1,

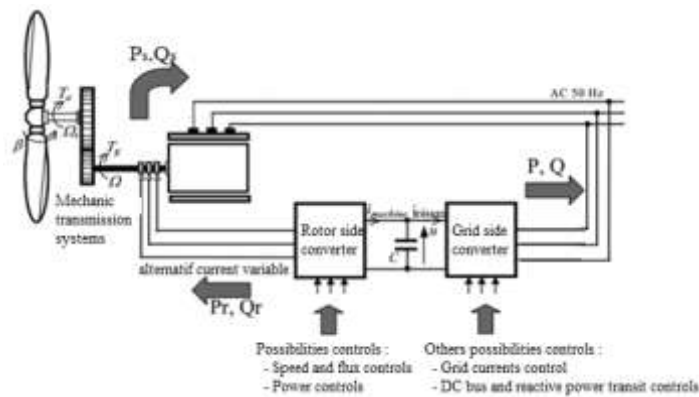


Figure 1 : The different possibilities control of the machine

B. State representation in the multivariate system

The machine state space model with voltageframe orientation is,

- The state vector is

$$x^T = (i_{rd} \quad i_{rq} \quad \phi'_{sd} \quad \phi'_{sq})$$

- The input vector on the stator side is $u_s^T = (u_{sd} \quad u_{sq})$

- The input vector on the rotor side is $u_r^T = (u_{rd} \quad u_{sq})$

The matrixsystem A_s , the matrix input of the rotor B_r and the input matrix of the stator B_s are written [5]:

$$A = \begin{pmatrix} -\frac{1}{\sigma} \left(\frac{1}{\tau_r} + \frac{1-\sigma}{\tau_s} \right) & \omega_r & \frac{1-\sigma}{\sigma \tau_s} & -\frac{1-\sigma}{\sigma} \omega \\ -\omega_r & -\frac{1}{\sigma} \left(\frac{1}{\tau_r} + \frac{1-\sigma}{\tau_s} \right) & \frac{1-\sigma}{\sigma} \omega & \frac{1-\sigma}{\sigma \tau_s} \\ \frac{1}{\tau_s} & 0 & -\frac{1}{\tau_s} & \omega_s \\ 0 & \frac{1}{\tau_s} & -\omega_s & -\frac{1}{\tau_s} \end{pmatrix}$$

$$B_s = \begin{pmatrix} -\frac{1-\sigma}{\sigma L_m} & 0 \\ 0 & -\frac{1-\sigma}{\sigma L_m} \\ \frac{1}{L_m} & 0 \\ 0 & \frac{1}{L_m} \end{pmatrix} \quad B_r = \begin{pmatrix} \frac{1}{\sigma L_r} & 0 \\ 0 & \frac{1}{\sigma L_r} \\ 0 & 0 \\ 0 & 0 \end{pmatrix}$$

(2)

The state space block diagrams of the system are represented in linear form.

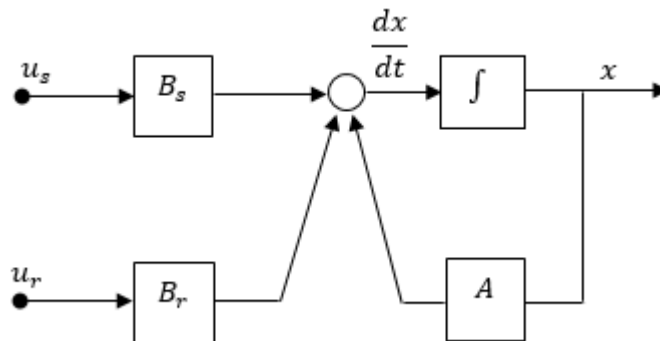


Figure 2 : Linear State Space Model of DFIM

The model can be written in the following form: $A = \begin{pmatrix} A_{11} & A_{12} \\ A_{21} & A_{22} \end{pmatrix} B_s = \begin{pmatrix} B_{s1} \\ B_{s2} \end{pmatrix} B_r = \begin{pmatrix} B_{r1} \\ 0 \end{pmatrix}$ (3)

The command synoptic diagram can be reproduced in more detail in the form of partial matrices,

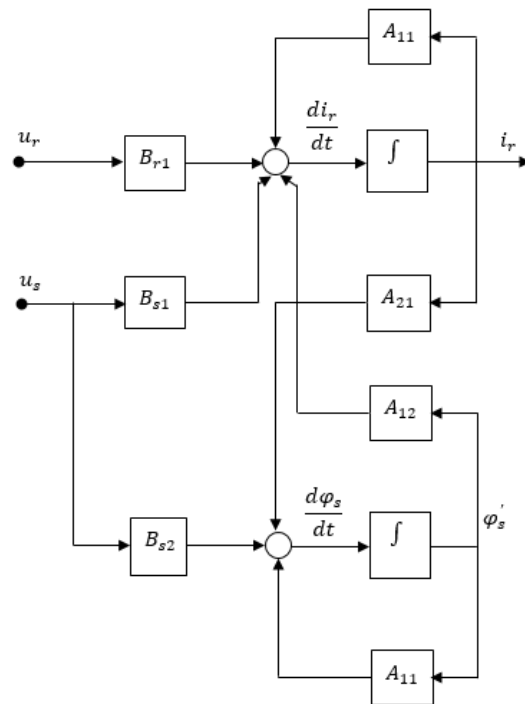


Figure 3 : Machine state space model in more detailed diagram form

The machine fluxstate representation is represented according to the state space equation:

$$\dot{x} = \begin{bmatrix} \dot{\phi}_{sd}(t) & \dot{\phi}_{sq}(t) & \dot{\phi}_{rd}(t) & \dot{\phi}_{rq}(t) \end{bmatrix}^T$$

$x = \begin{bmatrix} i_{sd} & i_{sq} & i_{rd} & i_{rq} \end{bmatrix}^T$ is the state of the system

$e = \begin{bmatrix} v_{sd} & v_{sq} & v_{rd} & v_{rq} \end{bmatrix}^T$ is the flux controls

$y = \begin{bmatrix} P_s & Q_s \end{bmatrix}^T$: the output

C. APPLICATIONS OF THE THEORY OF ROBUST CONTROL TO THE SYSTEM

We consider the system defined in figure 4, we must design a regulator which minimizes the norm of the transfer function from w to z . [6], [7], [8]

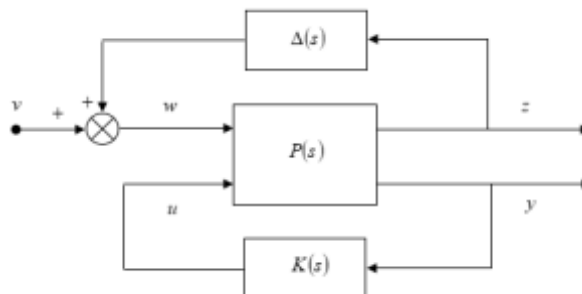


Figure 4 :Regulator which minimizes the norm H_2 and H_∞

The process $P(s)$ has the following realization:

$$\begin{aligned} \dot{x} &= Ax(t) + B_1w(t) + B_2u(t) \\ z(t) &= C_1x(t) + D_{11}w(t) + D_{12}u(t) \\ y(t) &= C_2x(t) + D_{21}w(t) + D_{22}u(t) \end{aligned} \quad (4)$$

The state space representation of the P(s) interconnection matrix is

$$\begin{bmatrix} \dot{x}(t) \\ e(t) \\ y(t) \end{bmatrix} = \begin{bmatrix} A & B_w & B_u \\ C_e & D_{ew} & D_{eu} \\ C_y & D_{yw} & D_{yu} \end{bmatrix} \begin{bmatrix} x(t) \\ w(t) \\ u(t) \end{bmatrix} \quad (5)$$

We also have another realization of P(s) like the following

$$P(s) = \begin{bmatrix} A & B_1 & B_2 \\ C_1 & D_{11} & D_{12} \\ C_2 & D_{21} & D_{22} \end{bmatrix} = \begin{bmatrix} P_{11}(s) & P_{12}(s) \\ P_{21}(s) & P_{22}(s) \end{bmatrix} \quad (6)$$

The transfer function of the regulated system with a K(s) regulator can be achieved

$$\begin{bmatrix} Z(s) \\ Y(s) \end{bmatrix} = \begin{bmatrix} P_{11}(s) & P_{12}(s) \\ P_{21}(s) & P_{22}(s) \end{bmatrix} \begin{bmatrix} W(s) \\ U(s) \end{bmatrix} \quad (7)$$

Determine K(s) stabilizing the loop system according to figure 5, while ensuring:

$$\|F_l(P(s), K(s))\|_\infty < \gamma \quad (8)$$

III. RESULTATS

The robust control of multivariable systems makes it possible to achieve the results presented below, according to the following numerical data [1]:

Vitesse de synchronisme [tr/min]	1500
Puissance évaluée [kW]	2000
Tension de ligne-tension du stator [V _{rms}]	690
Courant du stator [A _{rms}]	1760
Couple [Nm]	12732
Connection du stator	Etoile
p	2
u	0.34
R _s [Ω]	2.6
L _{σs} [H]	0.087
L _m [mH]	2.5
R _r ' [mΩ]	26.1
L _{σr} ' [mH]	0.738
R _r [mΩ]	2.9
L _{σr} [mH]	0.087
L _s [mH]	2.587
L _r [mH]	2.587

- The MADA operates in generator mode, confronted with different operating conditions, according to the wind speed parameters. The nominal torque is presented.

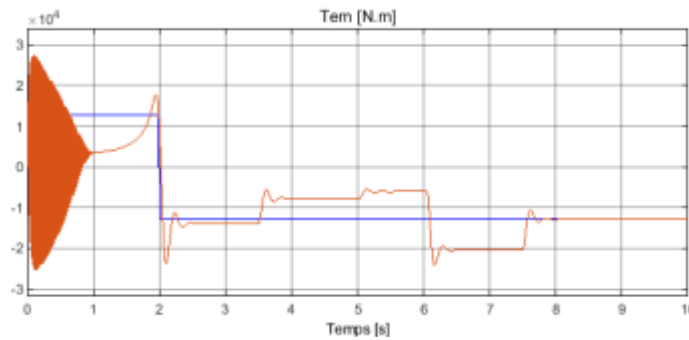


Figure 5 : Electromagnetic torque set according to the variation in wind speed

- In the figure showing the generator speed behavior, whatever the wind blast speed variation, the generator rotation speed never deviates far enough from the set speed (always around of 157.14 rad / s or 1500 rpm).

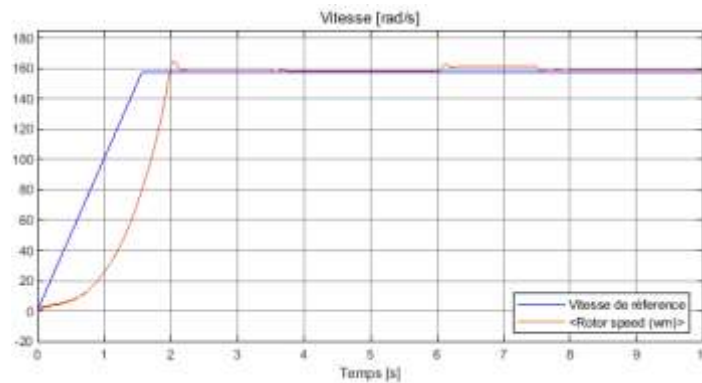


Figure 6 : Double-fed asynchronous generator speed curves set by the wind blast speed variations

The following figure represents the stator currents dq behavior.

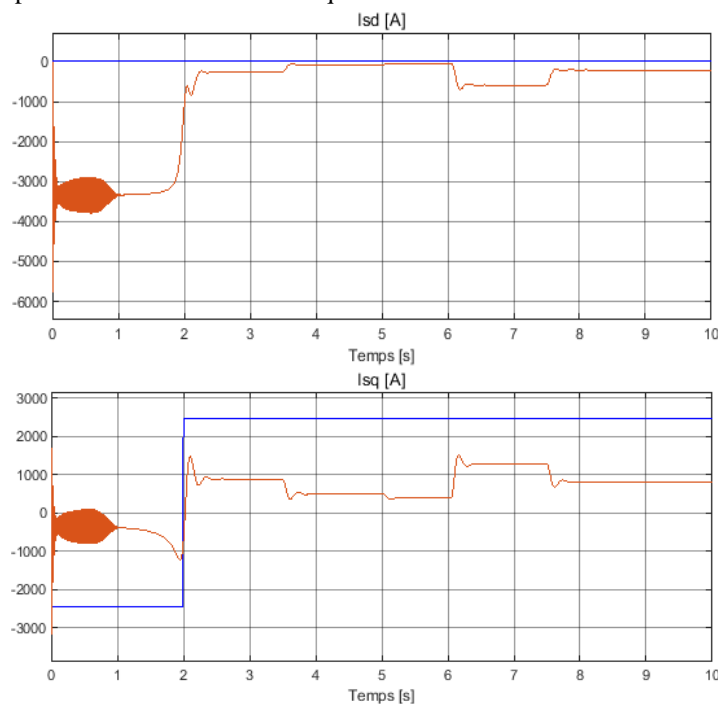


Figure 7 : The stator currents behavior parameterized according to the wind blast speed variations

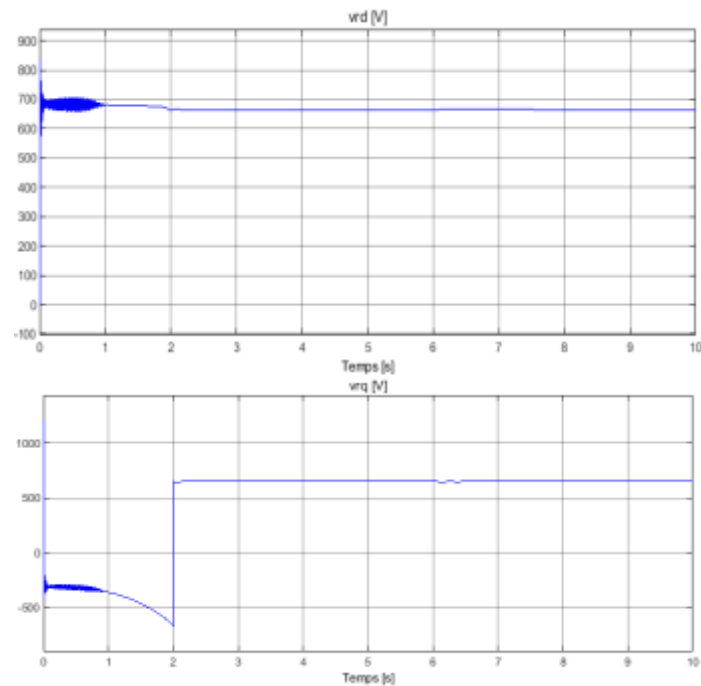


Figure 8 : Behavior of the control voltages in dq

In this figure below, the three-phase rotor currents are shown, the amplitude and frequency of these currents vary according to the values of the variations in wind blast speed.

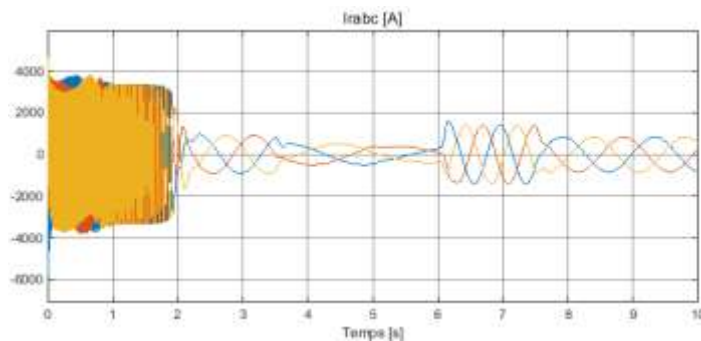


Figure 9 : Variations in the amplitude and frequency of the rotor current set according to the wind speed

On the other hand, in the figure below, the three-phase stator currents are represented, the amplitude of these currents vary according to the values of the variations of wind blast, but the frequency remains unchanged (always constant).

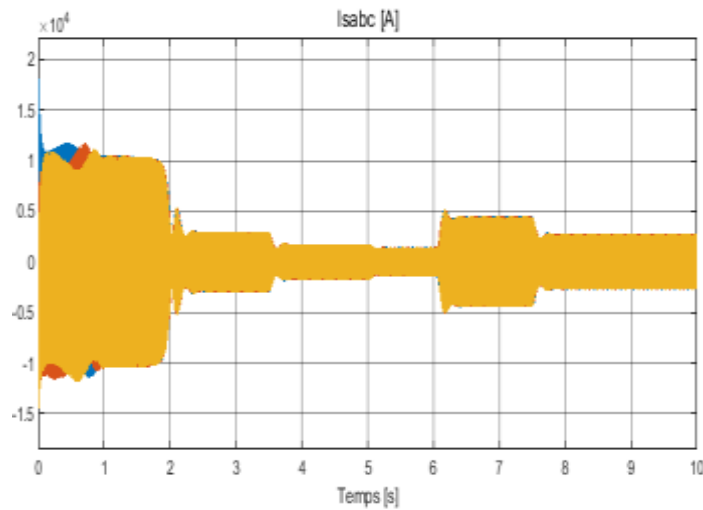


Figure 10 : Variations in the amplitude of the stator currents at constant frequency parameterized according to the wind speed

Whatever the variations in the various characteristics and parameters of its operation, the voltages obtained at the stator (outputs) always have the same frequencies as the network currents, and the amplitudes always follow the setpoint or reference values.

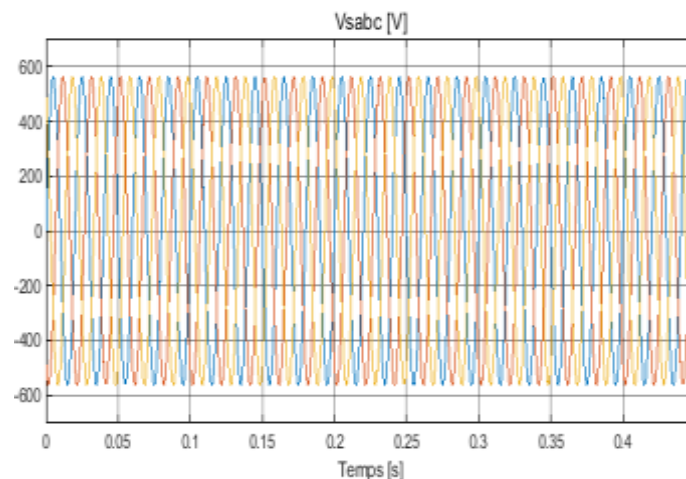


Figure 11 : Stator voltages set by wind speeds

IV. CONCLUSION

The specificity of the double-fed asynchronous machine is demonstrated [9], [10] according to these results presented by these figures, simulated in MATLAB, they show that if we want to control the system, in such a way that when the wind is blowing at very high speeds, a sensor will keep the speed of the turbine within the range of maximum speed that the machine could withstand. And if the wind speed is very low, a sensor will ask the system to supply a current via the network or an electric power generator to run the machine giving a speed regime so that the turbine can stay in the range of minimum speed range.

REFERENCES

- [1]. G. ABAD, J. LÓPEZ, A. MIGUEL RODRÍGUEZ, L. MARROYO, G. IWANSKI, 2016. Doubly fed induction machine, modeling and control for wind energy generation. Ieee Series.
- [2]. X. DEHONG, F. BLAABJERG, C. WENJIE, and N. ZHU. Advanced Control of Doubly Fed Induction Generator for Wind Power Systems, First Edition. © 2018 by The Institute of Electrical and Electronics Engineers, Inc. Published 2018 by John Wiley & Sons, Inc.
- [3]. GIRI, FOUAD, 2013. Ac electric engine control advanced design of techniques and applications.

- [4]. IWANSKI, Gonzalo A., 2014. Properties and control of a doubly fed induction machine in Power Electronics for Renewable Energy Systems, Transportation and Industrial Application. John Wiley & Sons
- [5]. N. PHUNG QUANG and J.-A. DITTRICHN, Vector Control of Three-Phase AC Machines,
- [6]. F. LIN, 2007 Robust Control Design, an Optimal Control Approach.
- [7]. Da-Wei GU, P. H. PETKOV M. M. KONSTANTINOV, 2013. Robust Control Design with MATLAB®.
- [8]. G. Rigatos, 2016. Intelligent Renewable Energy Systems, © Springer International Publishing Switzerland.
- [9]. H.t RAZIK, 2011. Handbook of Asynchronous Machine with Variable Speed.
- [10]. ZHOU, DAO, SONG, YIPENG; BLÅBJERG, FREDE, 2016. Modern control strategies of doubly-fed induction generator based wind turbine system, Published in: Chinese Journal of Electrical Engineering.